Dynamical Lamb effect in a superconducting circuit

Mirko Amico, Oleg L. Berman, and Roman Ya. Kezerashvili

Phys. Rev. A **100**, 013841 — Published 22 July 2019

DOI: 10.1103/PhysRevA.100.013841

Dynamical Lamb effect in a superconducting circuit

Mirko Amico[1,2], Oleg L. Berman[1,2] and Roman Ya. Kezerashvili[1,2]
[1] *Physics Department, New York City College of Technology, The City University of New York, Brooklyn, NY 11201, USA*
[2] *The Graduate School and University Center, The City University of New York, New York, NY 10016, USA*

The dynamical Lamb effect is predicted to arise in superconducting circuits when the coupling of a superconducting qubit with a resonator is periodically switched "on" and "off" nonadiabatically. We show that by using a superconducting circuit which allows to switch between longitudinal and transverse coupling of a qubit to a resonator, it is possible of to observe the dynamical Lamb effect. The switching between longitudinal and transverse coupling can be achieved by modulating the magnetic flux through the circuit loops. By solving the Schrödinger equation for a qubit coupled to a resonator, we calculate the time-evolution of the number of excitations in the qubit and the resonator due to the dynamical Lamb effect. The number of excitations created in the system is maximum when the coupling is periodically switched between longitudinal and transverse using a square-wave or sinusoidal modulation of the magnetic flux with frequency equal to the sum of the average qubit and photon transition frequencies.

PACS numbers:

I. INTRODUCTION

According to quantum field theory, the vacuum is filled with virtual particles which can be turned into real ones by specific external perturbations [1]. Phenomena of this kind are commonly referred to as quantum vacuum phenomena. Several quantum vacuum phenomena related to the peculiar nature of the quantum vacuum have been predicted [2–4], some of which, as the Lamb shift [5] and the Casimir effect [2], have been experimentally found [6–11]. Other examples of quantum vacuum phenomena include the dynamical Casimir effect (DCE) [12], that is the creation of real photons from the vacuum, and the dynamical Lamb effect (DLE) [13], which is the excitation of an atom in a cavity, along with the creation of photons. Both the DCE and the DLE arise due to the fast change in boundary conditions of a cavity. The dynamical Lamb effect was first encountered in Ref. [13], where the situation of an atom passing through a cavity at relativistic speed was considered. In this case, the excitation of the atom and the generation of photons was thought to arise because of the sudden change of Lamb shift of the atom. Therefore, the phenomenon was called dynamical Lamb effect. In Ref. [14], the same setup of an atom in its ground-state accelerating through a cavity is considered. There, the DLE was understood as an enhanced generation of thermal radiation due to the nonadiabatic effects at the cavity boundary and termed cavity-enhanced Unruh effect [4]. Similarly to the dynamical Casimir effect, a nonadiabatic change in the boundary conditions of the cavity is required for the instantaneous change of the Lamb shift of the atom which generates the dynamical Lamb effect. However, this is very difficult to obtain in a setup with physical atoms and cavities.

Recently, the DCE has been experimentally observed in superconducting circuits [15, 16]. The latter provide a way to model atoms and cavities using Josephson junctions and superconducting transmission lines. The advantage of a superconducting circuit setup over real atoms and cavities lies in the possibility of tuning the parameters of the system in a short time-interval, allowing us to enter the nonadiabatic regime where the mentioned quantum vacuum phenomena may arise [17]. Following the case of the DCE, several proposals have been made for the observation of the DLE in superconducting circuits [18, 19]. In Ref. [18] it is suggested that by turning "on" and "off" the coupling of a superconducting qubit to a resonator, one can induce a sudden change in the Lamb shift of the qubit. While in Ref. [19], it was proposed that in a superconducting circuit with a qubit coupled to a resonator, the modulation of the qubit/resonator coupling strength can be used to mimic the situation of an atom passing through a cavity at relativistic speed. The proposals of Refs. [18] and [19] generated a number of following publications [20–27]. Both proposals lead to the quantum vacuum phenomena that we call dynamical Lamb effect. In fact, an atom entering a cavity at relativistic speed experiences an instantaneous change in its Lamb shift due to the nonadiabatic change in the electromagnetic environment surrounding it. The nonadiabatic effects arising in a system of a qubit coupled to a single-mode of the electromagnetic field were also studied in Ref. [28]. Similar results were obtained for a polaritonic system where time modulations of the vacuum Rabi frequency [29] were considered [30–32]. More specifically, enhanced production of photons was predicted for periodic modulations of the vacuum Rabi frequency. These results have also been extended to superconducting circuit setups [33–36], providing an open-system approach to the study of quantum vacuum phenomena arising due to time-dependent modulations of the system's parameters. In facts, the first experimental observation of a tunable Lamb shift was achieved in a superconducting circuit [37].

In Refs. [38, 39], it was shown that it is possible to design a superconducting circuit where the qubit/resonator coupling is switched between longitudinal and transverse by modulating the magnetic flux through the circuit loops. A qubit/resonator system longitudinally coupled can be seen as a decoupled system with renormalized energy levels [47]. Whereas in a qubit/resonator system with transverse coupling the qubit and the photons interact. Therefore, we suggest the possibility of observing the dynamical Lamb effect by adopting the circuit designed in Refs. [38, 39] and periodically switching between longitudinal and transverse qubit/resonator coupling. This effectively corresponds to periodically switching "on" and "off" of the qubit/resonator coupling, which has been shown to give rise to the dynamical Lamb effect [18].

To demonstrate the presence of the dynamical Lamb effect, we calculate the number of excitations in the qubit and the resonator by solving the Schrödinger equation. In a previous article [24], we used an open-system approach to the study of the dynamics of the system. The results showed that dissipation can be neglected when typical values of the parameters of the system are considered. This can be understood from the nonadiabatic nature of the phenomenon under study, which involves a much faster dynamic compared to the one characteristic of dissipative effects. Therefore, even though open-system approaches for the study of this problem exist, we do not deem it necessary for this case. The calculations show that the number of excitations in the qubit and resonator due to the dynamical Lamb effect reach its maximum values when the coupling is periodically switched between transverse and longitudinal using a square-wave or sinusoidal modulation of the magnetic flux with frequency equal to the sum of the average qubit and photon transition frequencies.

The article is organized as follows. In Sec. II the Hamiltonian of a qubit/resonator system with longitudinal or transverse coupling is described. In Sec. III, a superconducting circuit which allows for the switching between a longitudinally coupled Hamiltonian and a transverse one is introduced. We show how to switch between longitudinal and transverse coupling by modulating the magnetic flux threading the circuit. The results of numerical calculations of the time-evolution of the number of excitations in the qubit and the resonator for different modulation of the magnetic flux are given in Sec. IV. Conclusions follow in Sec. V.

II. LONGITUDINAL AND TRANSVERSE COUPLING

The possibility of switching between a transverse coupling scheme and a longitudinal one was proposed in Refs. [38, 39], but this was not envisioned as a fast switching which can lead to the observation of quantum vacuum phenomena. Furthermore, the proposal of a periodic switching "on" and "off" of the qubit/resonator coupling was originally made in Ref. [18] without any specific suggestions on how to exactly achieve this in practice. In fact, even though the ability of tuning the qubit/cavity coupling is well established in superconducting circuits [40–45], this usually entails a modification of the qubit's and resonator's transition frequencies. The latter would make it impossible to use a fixed frequency of switching "on" and "off" of the coupling that is resonant with the sum frequency of cavity and resonator transition frequencies. Adopting the circuit proposed in Refs. [38, 39] for this purpose allows to achieve this goal because the influence of the switching on the qubit and resonator's transition frequencies is small enough. In this paper we propose to achieve nonadiabatically fast periodic switching "on" and "off" of the qubit resonator coupling [18] by adopting the superconducting circuit proposed in Refs. [38, 39]. This allows us to achieve the parameters regime which satisfies the conditions necessary for the observation of the dynamical Lamb effect.

As a first step, let us show how a system with longitudinal qubit/resonator coupling can be seen as an uncoupled system, in contrast to the case of transverse qubit/resonator coupling. The Hamiltonians of a qubit longitudinally $\hat{H}_L$ and transversely $\hat{H}_T$ coupled to a resonator, respectively, can be written as

$$\hat{H}_L = \hbar\omega_0\hat{\sigma}^+\hat{\sigma}^- + \hbar\omega_r\hat{a}^\dagger\hat{a} + \hbar g_{zx}\hat{\sigma}_z\Big(\hat{a}^\dagger + \hat{a}\Big), \tag{1}$$

$$\hat{H}_T = \hbar\omega_0\hat{\sigma}^+\hat{\sigma}^- + \hbar\omega_r\hat{a}^\dagger\hat{a} + \hbar g_{xx}\hat{\sigma}_x\Big(\hat{a}^\dagger + \hat{a}\Big), \tag{2}$$

where ω_0 is the transition frequency of the qubit, ω_r is the frequency of the photons in the resonator, $\hat{\sigma}^+ = \frac{\hat{\sigma}_x + i\hat{\sigma}_y}{2}$, $\hat{\sigma}^- = \frac{\hat{\sigma}_x - i\hat{\sigma}_y}{2}$ and $\hat{a}^\dagger$, $\hat{a}$ are the creation and annihilation operators for excitations of qubit and photons, respectively, $\hat{\sigma}_x$, $\hat{\sigma}_y$ and $\hat{\sigma}_z$ are the Pauli x, y and z operators, while g_{zx} and g_{xx} are the longitudinal and transverse coupling strengths, respectively. The terms $\hat{\sigma}^+\hat{a}$ and $\hat{\sigma}^-\hat{a}^\dagger$ in Hamiltonian (2) conserve the number of excitations in the system and they are called rotating terms. While $\hat{\sigma}^-\hat{a}$ and $\hat{\sigma}^+\hat{a}^\dagger$ can decrease or increase the number of excitations in the system and they are called counter-rotating terms. Applying an appropriate unitary transformation [46, 47], the Hamiltonian (1) can be written in a diagonal form as

$$\hat{H}'_L = \hbar\omega_0\hat{\sigma}^+\hat{\sigma}^- + \hbar\omega_r\hat{a}^\dagger\hat{a} - \frac{\hbar^2 g_{zx}^2}{\omega_r}\hat{I}, \tag{3}$$

where $\hat{I}$ is the identity operator. Since $\hat{H}'_L$ and $\hat{H}_L$ are related by a unitary transformation, their eigenvalues are the same and they describe a qubit and a resonator with the same transition frequencies. Therefore, the two Hamiltonians describe systems which are characterized by the same observables. However, in (3) the qubit is now decoupled from the resonator and the zero-point energy is renormalized. In this case, the Lamb shift of the qubit is absent. In contrast, in the case of Hamiltonian (2) the qubit and the resonator cannot be decoupled by any sort of unitary transformation. The latter implies, for instance, that the energy levels of the qubit are affected by the Lamb shift. So, we can regard the system with longitudinal coupling given by Eq. (1) as a system of a qubit and a resonator with the qubit/resonator coupling turned "off" and the system with transverse coupling defined by Hamiltonian (2) as the same qubit and resonator with the qubit/resonator coupling turned "on". Thus, the switching between these two coupling regimes involves a change in the Lamb shift of the qubit.

III. SUPERCONDUCTING CIRCUIT WITH TUNABLE QUBIT/RESONATOR COUPLING

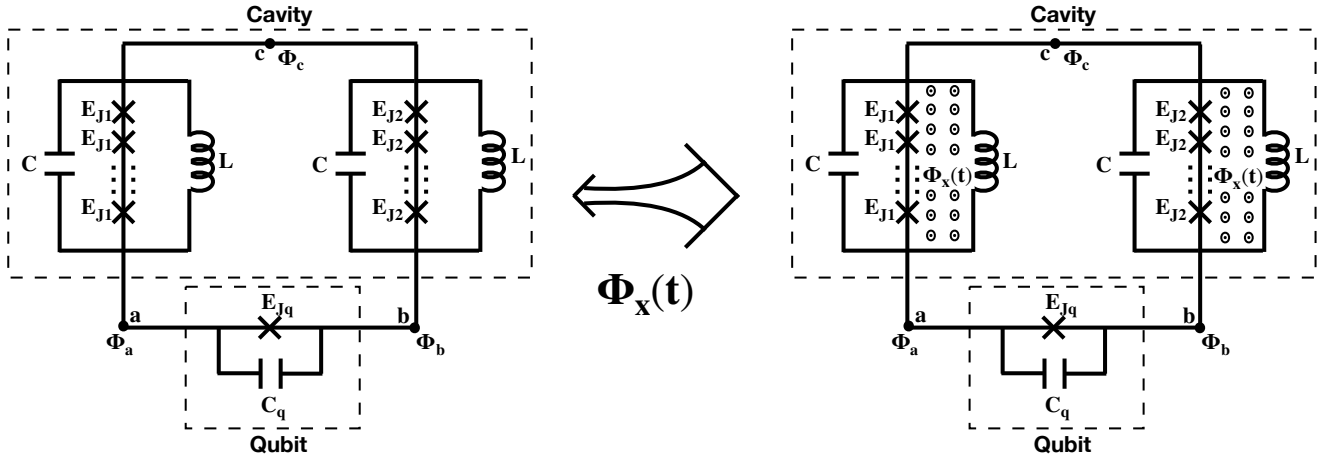

FIG. 1: Superconducting circuit for a qubit coupled to a resonator with tunable qubit/resonator coupling. By turning "on" and "off" the magnetic flux $\Phi_x(t)$ we can switch between a description of the circuit in terms of a transversely coupled Hamiltonian and a longitudinal one.

Let us consider the circuit in Fig. 1 and define the branch fluxes associated with the qubit and the resonator, as $\Phi_q = \Phi_a - \Phi_b$ and $\Phi_r = \Phi_a + \Phi_b - 2\Phi_c$, respectively, where Φ_a, Φ_b and Φ_c are the magnetic fluxes at the nodes a, b and c. Following Ref. [48], one can write the Lagrangian for the circuit in Fig. 1 by adding the contributions of each element in terms of the branch fluxes [39]

$$\begin{aligned}\mathcal{L} = &\left(\frac{2C_q + C}{4}\dot{\Phi}_q^2 + \frac{C}{2}\dot{\Phi}_r^2\right) - \frac{1}{4L}\left(\Phi_q^2 + \Phi_r^2\right) + E_{J_q}\cos\left(\frac{2\pi}{\Phi_0}\Phi_q\right) + \\ &+ kE_{J1}\cos\left(\frac{2\pi}{\Phi_0}\left(\frac{\Phi_q + \Phi_r}{2k} + \frac{\Phi_x(t)}{k}\right)\right) + kE_{J2}\cos\left(\frac{2\pi}{\Phi_0}\left(\frac{\Phi_q - \Phi_r}{2k} + \frac{\Phi_x(t)}{k}\right)\right).\end{aligned} \tag{4}$$

In Eq. (4), $\Phi_x(t)$ is the external magnetic flux threading the areas enclosed by the left and right loops, k is the number of Josephson junctions in a branch of the circuit, which the same in each branch, C and L are the capacitance and the inductance of the loops, respectively, E_{J1} and E_{J2} are the Josephson energies of the junctions in each branch, E_{Jq} the Josephson energy of the qubit junction and C_q its capacitance. The Hamiltonian of the system can be found by taking the Legendre transform of the Lagrangian: $\mathcal{H} = \sum_{i=1}^{N}\frac{d\mathcal{L}}{d\dot{\Phi}_i}\dot{\Phi}_i - \mathcal{L}$, where $i = q, r$ are the indices corresponding to the qubit and resonator flux variables, respectively. This leads to the following Hamiltonian for the circuit

$$\mathcal{H}(t) = \frac{1}{2C_q + C} Q_q^2 + \frac{1}{C} Q_r^2 + \frac{1}{4L}\left(\Phi_q^2 + \Phi_r^2\right) - E_{J_q} \cos\left(\frac{2\pi}{\Phi_0}\Phi_q\right) + \\ -kE_{J1} \cos\left(\frac{2\pi}{\Phi_0}\left(\frac{\Phi_q + \Phi_r}{2k} + \frac{\Phi_x(t)}{k}\right)\right) - kE_{J2} \cos\left(\frac{2\pi}{\Phi_0}\left(\frac{\Phi_q - \Phi_r}{2k} + \frac{\Phi_x(t)}{k}\right)\right). \tag{5}$$

A quantum mechanical model of the circuit can be obtained from its classical Hamiltonian by applying the standard procedure of second quantization for the qubit and resonator variables separately [39]. Let us first consider the quantization of resonator variables by setting $Q_q = 0$, $\Phi_q = 0$ and $\Phi_x = 0$. If the sum of the Josephson energies kE_{J1} and kE_{J2} of the two junction arrays is much greater than the charging energy $E_c = \frac{e^2}{2C}$, where C is the capacitance in parallel to each array of junctions, the cosine potential energy term in Eq. (5), for small values of Φ_r, can be well approximated by a harmonic potential [38, 49]. For the specific values of the parameters of the circuit chosen in Sec. IV (see Eq. (16)) we have $kE_{J1} = h \times 734.4$ GHz, $kE_{J2} = h \times 705.6$ GHz and $E_c = h \times 189.9$ MHz. Therefore, $kE_{J1} + kE_{J2} \gg E_c$ by about four orders of magnitude. Thus, expanding the cosine in terms of Φ_r up to second order, and expressing the resonator's variables Q_r and Φ_r in terms of the operators of creation $\hat{a}^\dagger$ and annihilation $\hat{a}$ of photons in the resonator as

$$Q_r = \left(\left(\frac{\hbar}{2}\right)^2 \frac{C(1+\eta)}{L}\right)^{\frac{1}{4}} i\left(\hat{a}^\dagger - \hat{a}\right), \qquad \Phi_r = \left(\hbar^2 \frac{L}{C(1+\eta)}\right)^{\frac{1}{4}} \left(\hat{a} + \hat{a}^\dagger\right), \tag{6}$$

we obtain

$$\hat{\mathcal{H}}_r = \hbar\omega_r \left(\hat{a}^\dagger \hat{a} + \frac{1}{2}\right). \tag{7}$$

In Eq. (7) $\omega_r = \sqrt{\frac{1+\eta}{LC}}$ is the transition frequency between the energy levels of the system and η is a dimensionless parameter defined in Table II. This parameter accounts for the flux-dependence of the system. The Hamiltonian (7) is the Hamiltonian of a harmonic oscillator. The operators of creation and annihilation of photons in the resonator are bosonic operators which satisfy the commutation relation $\left[\hat{a}, \hat{a}^\dagger\right] = 1$. With the definitions given in Eq. (6), and the commutation relation for $\hat{a}^\dagger$ and $\hat{a}$, one can prove that the variables Φ_r and Q_r satisfy the commutation relation for conjugate variables $[\Phi_r, Q_r] = i\hbar$. Let us now turn back and consider the quantization of qubit variables. Starting from Hamiltonian (5), we set $Q_r = 0$, $\Phi_r = 0$ and $\Phi_x = 0$ and expand the cosine in terms of Φ_q up to second order [49]. This can be done because the above mentioned Josephson energies kE_{J1}, kE_{J2} and $E_{Jq} = h \times 10$ GHz are at least two orders of magnitude greater than the charging energy $E_c = \frac{e^2}{2(C_q + C)} = h \times 119.6$ MHz, for the values of the parameters of the circuit chosen in Sec. IV, Eq. (16). Then, introducing the operators of creation $\hat{b}^\dagger$ and annihilation $\hat{b}$ of qubit excitations in terms of Q_q and Φ_q,

$$Q_q = e\left(\left(E_{Jq} + \left(\frac{\Phi_0}{2\pi}\right)^2 \frac{1+\eta}{2L}\right)\frac{2C_q + C}{2e^2}\right)^{\frac{1}{4}} i\left(\hat{b}^\dagger - \hat{b}\right), \qquad \Phi_q = \left(\frac{\Phi_0}{2\pi}\right)\left(\frac{2e^2}{2C_q + C}\frac{1}{E_{Jq} + \left(\frac{\Phi_0}{2\pi}\right)^2 \frac{1+\eta}{2L}}\right)^{\frac{1}{4}} \left(\hat{b} + \hat{b}^\dagger\right), \tag{8}$$

we obtain the following quantum mechanical Hamiltonian

$$\hat{\mathcal{H}}_q = \hbar\omega_q \left(\hat{b}^\dagger \hat{b} + \frac{1}{2}\right). \tag{9}$$

In Eq. (9) $\omega_q = \frac{\sqrt{8\left(E_{Jq} + \left(\frac{\Phi_0}{2\pi}\right)^2 \frac{1+\eta}{2L}\right)\frac{2e^2}{2C_q + C}}}{\hbar}$ is the transition frequency between the first two energy levels of the system. The operators of creation and annihilation of qubit excitations are also taken to be bosonic operators satisfying the commutation relation $\left[\hat{b}, \hat{b}^\dagger\right] = 1$. Again, one can prove that the variables Φ_q and Q_q satisfy the commutation relation for conjugate variables $\left[\Phi_q, Q_q\right] = i\hbar$ by using the commutation relation for $\hat{b}^\dagger$ and $\hat{b}$, together with the definitions

TABLE I: Instantaneous values of the parameters given in Table II for the case of square-wave modulation of the external magnetic flux Φ_x.

Transverse coupling: $\Phi_x = 0$	Longitudinal coupling: $\Phi_x = \frac{k\pi}{2}$
$\eta^T = \frac{E_{J1}+E_{J2}}{2k}\left(\frac{2\pi}{\Phi_0}\right)^2 L$	$\eta^L = 0$
$E_{Jq}^{*T} = E_{Jq} + \left(\frac{\Phi_0}{2\pi}\right)^2 \frac{1+\eta^T}{2L}$	$E_{Jq}^{*L} = E_{Jq} + \left(\frac{\Phi_0}{2\pi}\right)^2 \frac{1}{2L}$
$\omega_r^T = \sqrt{\frac{1+\eta^T}{LC}}$	$\omega_r^L = \sqrt{\frac{1}{LC}}$
$\omega_0^T = \sqrt{8E_c E_{Jq}^{*T}} - E_c \frac{E_{Jq}+\left(\frac{\Phi_0}{2\pi}\right)^2 \frac{\eta^T}{2k^2 L}}{E_{Jq}^{*T}}$	$\omega_0^L = \sqrt{8E_c E_{Jq}^{*L}} - E_c \frac{E_{Jq}}{E_{Jq}^{*L}}$
$g_{xx}^T = \frac{E_{J1}-E_{J2}}{2k^2}\sqrt[4]{\frac{2E_C}{E_{Jq}^{*T}}}\frac{\pi}{\Phi_0}\sqrt[4]{\frac{L}{C}\frac{1}{1+\eta^T}}$	$g_{xx}^L = 0$
$g_{zz}^T = -\frac{E_{J1}-E_{J2}}{16\,k^3}\sqrt{\frac{2E_C}{E_{Jq}^{*T}}}\left(\frac{\pi}{\Phi_0}\right)^2\sqrt{\frac{L}{C}\frac{1}{1+\eta^T}}$	$g_{zz}^L = 0$
$g_{zx}^T = 0$	$g_{zx}^L = -\frac{E_{J1}-E_{J2}}{8\,k^2}\sqrt{\frac{2E_C}{E_{Jq}^{*L}}}\frac{\pi}{\Phi_0}\sqrt[4]{\frac{L}{C}}$
$g_{xz}^T = 0$	$g_{xz}^L = -\frac{E_{J1}-E_{J2}}{4\,k^2}\sqrt[4]{\frac{2E_C}{E_{Jq}^{*L}}}\left(\frac{\pi}{\Phi_0}\right)^2\sqrt{\frac{L}{C}}$

given in Eq. (8). The energy levels of the system for a weakly anharmonic potential are not all equally spaced and by addressing the system at the right frequency one can induce transitions between two levels alone [50]. Therefore, we consider only two accessible levels, namely the ground and the first excited state, and replace the creation and annihilation operators $\hat{b}$ and $\hat{b}^\dagger$, respectively, with $\hat{\sigma}^+$ and $\hat{\sigma}^-$. The latter ones are used to describe excitations in a two-level system. The transition frequency between the first two levels is also adjusted to take into account the anharmonicity by replacing ω_q with ω_0. Therefore, we rewrite the Hamiltonian (9) as

$$\hat{\mathcal{H}}_q' = \hbar\omega_0\left(\hat{\sigma}^+\hat{\sigma}^- + \frac{1}{2}\right), \tag{10}$$

Hamiltonian (10) is the Hamiltonian of a quantum two-level system. To obtain a quantum mechanical Hamiltonian of the system, one can substitute the expressions for the resonator and qubit variables given in Eqs. (6) and (8), respectively, into Hamiltonian (5). In this way, one can also express the terms in Hamiltonian (5) which involve both resonator and qubit variables in the argument of the cosine, thus coupling those variables, in terms of creation and annihilation operators of the photons excited in the resonator and the qubit's excitation. Thus, getting

$$\begin{aligned}\hat{\mathcal{H}}(t) = \hbar\omega_r(t)\left(\hat{a}^\dagger\hat{a} + \frac{1}{2}\right) + \hbar\frac{\omega_0(t)}{2}\hat{\sigma}_z + \hbar g_{xx}(t)\hat{\sigma}_x\left(\hat{a}^\dagger + \hat{a}\right) + \hbar g_{zz}(t)\hat{\sigma}_z\left(\hat{a}^\dagger + \hat{a}\right)^2 + \\ + \hbar g_{zx}(t)\hat{\sigma}_z\left(\hat{a}^\dagger + \hat{a}\right) + \hbar g_{xz}(t)\hat{\sigma}_x\left(\hat{a}^\dagger + \hat{a}\right)^2,\end{aligned} \tag{11}$$

where $\omega_r(t)$ is the transition frequency of the resonator, $\omega_0(t)$ is the transition frequency of the qubit and $g_{xx}(t)$, $g_{zz}(t)$, $g_{zx}(t)$ and $g_{xz}(t)$ are the coupling strengths. The expressions of each of the parameters in Hamiltonian (11) are given in Table II in the Appendix. It is important to note that all these parameters depend on time through their dependence on the external magnetic flux $\Phi_x(t)$.

A. Square-wave modulation

We consider two forms of the magnetic flux modulation: a square-wave and a sinusoidal one. Let us first focus on the case of a square-wave modulation of the magnetic flux

$$\Phi_x(t) = \frac{k\pi}{2}\theta\left(\cos\left(\varpi_s t + \frac{3\pi}{2}\right)\right), \tag{12}$$

where $\theta(\cdot)$ is the Heaviside function which switches on periodically with period $T_s = 1/\varpi_s$, where ϖ_s is the frequency of the switching of the magnetic flux. By switching the external magnetic flux $\Phi_x(t)$ between the values 0 and $\frac{k\pi}{2}$,

one can tune the qubit and the resonator parameters in Hamiltonian (11) at each instant of time. This gives the instantaneous switching between transverse and longitudinal qubit/resonator coupling which can be used to give rise to the dynamical Lamb effect. Although this kind of modulation is closest to the ideal situation of instantaneous switching, it can be difficult to achieve with the experimental instruments available now because of the short period T_s of the square wave required.

In particular, for $\Phi_x = 0$ we can write the Hamiltonian (11) as

$$\hat{\mathcal{H}}_T = \hbar\omega_r^T\left(\hat{a}^\dagger\hat{a} + \frac{1}{2}\right) + \hbar\frac{\omega_0^T}{2}\hat{\sigma}_z + \hbar g_{xx}^T\hat{\sigma}_x\left(\hat{a}^\dagger + \hat{a}\right) + \hbar g_{zz}^T\hat{\sigma}_z\left(\hat{a}^\dagger + \hat{a}\right)^2, \tag{13}$$

where the expression of the parameters $\left\{\omega_r^T, \omega_0^T, g_{xx}^T, g_{zz}^T\right\}$ are given in Table I. In this case, $\{g_{xx}, g_{zz} \neq 0; g_{zx}, g_{xz} = 0\}$ and the Hamiltonian (13) is instantaneously equivalent to the Hamiltonian (2) of a transversely coupled qubit/resonator system, with the exception of an extra coupling term.

On the other hand, for $\Phi_x = \frac{k\pi}{2}$, Hamiltonian (11) can be reduced to the following form

$$\hat{\mathcal{H}}_L = \hbar\omega_r^L\left(\hat{a}^\dagger\hat{a} + \frac{1}{2}\right) + \hbar\frac{\omega_0^L}{2}\hat{\sigma}_z + \hbar g_{zx}^L\hat{\sigma}_z\left(\hat{a}^\dagger + \hat{a}\right) + \hbar g_{xz}^L\hat{\sigma}_x\left(\hat{a}^\dagger + \hat{a}\right)^2, \tag{14}$$

where the expressions of $\left\{\omega_r^L, \omega_0^L, g_{xx}^L, g_{zz}^L\right\}$ are also given in Table I. Here, $\{g_{xx}, g_{zz} = 0; g_{zx}, g_{xz} \neq 0\}$, which leads to an instantaneous longitudinal qubit/resonator coupling as in (1), with a spurious coupling term. To suppress the unwanted terms g_{zz}^T and g_{xz}^L in Hamiltonian (13) and (14), respectively, we choose specific values of the parameters of the circuit.

B. Sinusoidal modulation

While the square-wave modulation of the magnetic flux $\Phi_x(t)$ comes closest to the requirement of periodic and instantaneous switching "on" and "off" of the qubit/resonator coupling needed to observe the dynamical Lamb effect, this may be difficult to achieve in a realistic experimental setting. For this reason, we turn to another type of modulation, a sinusoidal one, which can be easily obtained in experiments. In fact, a high-frequency sinusoidal magnetic flux was used in the first experimental observation of the dynamical Casimir effect [15]. This models the more realistic situation where a finite amount of time is needed to switch "on" and "off" the coupling of the qubit with the resonator. Thus, we take $\Phi_x(t)$ as

$$\Phi_x(t) = \frac{k\pi}{2}\left(\frac{1}{2} + \frac{1}{2}\cos(\varpi_s t)\right). \tag{15}$$

In this case, the magnetic flux doesn't instantaneously switch "on" and "off" but continuously increases or decreases to its maximum or minimum value, respectively. However, the rise time $t_{\text{rise}} = t\left(\Phi_x = \frac{k\pi}{2}\right) - t(\Phi_x = 0)$, that is the time required to increase the magnetic flux from the minimum value to the maximum value, and, vice versa, the fall time $t_{\text{fall}} = t(\Phi_x = 0) - t\left(\Phi_x = \frac{k\pi}{2}\right)$, the time needed to decrease it from the maximum value to the minimum value, are shorter than any parameter with dimension of time ($t_{\text{rise}}, t_{\text{fall}} \ll \omega_0^{-1}, \omega_r^{-1}$). Therefore, one can still consider this modulation to be nonadiabatic. The parameters of Hamiltonian (11) do not take the simple form shown in Table I for the case of square-wave modulation but vary continuously with the magnetic flux $\Phi_x(t)$. These parameters can be found by substituting the sinusoidal modulation of the magnetic flux in the corresponding expressions from Table II in the Appendix.

IV. RESULTS AND DISCUSSION

We numerically solve the Schrödinger equation for the Hamiltonian (11) in the case of periodic switching between transverse and longitudinal coupling with the initial condition $|\psi(t = 0)\rangle = |g, 0\rangle$, where g denotes the qubit in the ground state and 0 is the number of photons in the resonator. In the numerical calculations of the number of excitations in the qubit and resonator, we use the following values of the parameters of the circuit [39]:

$$
\begin{aligned}
&k = 9, && E_{Jq} = h \times 10 \text{ GHz}, \\
&E_{J1} = h \times 81.6 \text{ GHz}, && E_{J2} = h \times 78.4 \text{ GHz}, \\
&C = 102 \text{ fF}, && C_q = 60 \text{ fF}, \\
&L = 5 \text{ nH}.
\end{aligned}
\tag{16}
$$

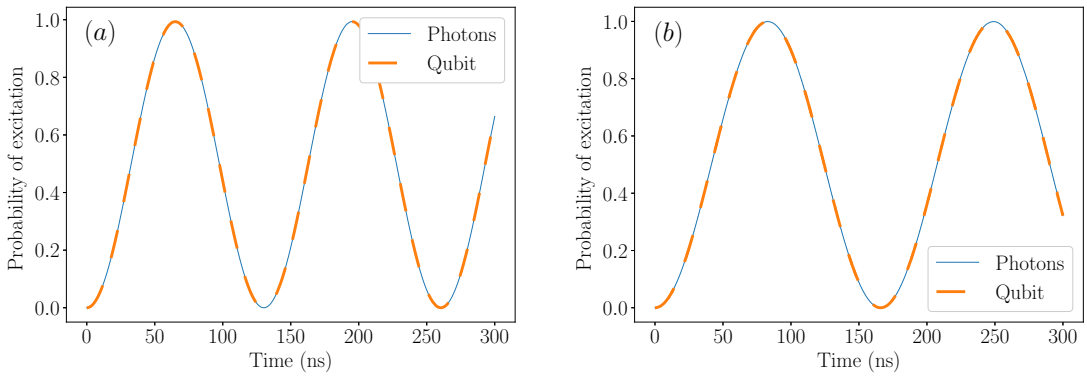

FIG. 2: Time dependence of the number of excitations in the qubit and the resonator for a frequency of switching of the magnetic flux $\varpi_s = \bar{\omega}_r + \bar{\omega}_0$ for a square-wave modulation (a) and a sinusoidal modulation (b) of the magnetic flux.

The results of our calculations are presented in Figs. 2 and 3. In Figs. 2a and 2b the time-dependence of the expected number of excitations in the qubit and the resonator for a square-wave and a sinusoidal modulation of the coupling is presented. The plots shown correspond to specific values of the frequency of switching ϖ_s of the magnetic flux for the two different type of modulation. In both cases, the value of the frequency of switching of the magnetic flux which maximize the number of excitations in the qubit and the resonator is $\varpi_s = \bar{\omega}_r + \bar{\omega}_0$, which is the sum of the time-averaged qubit transition frequency $\bar{\omega}_0 = \frac{1}{T}\int_0^T \omega_0(t')dt'$ and the time-averaged photon transition frequency $\bar{\omega}_r = \frac{1}{T}\int_0^T \omega_r(t')dt'$ over a period of oscillation of the magnetic flux. Because of the different time-dependence of the qubit and resonator transition frequencies for the different modulations, the number of excitations in the qubit and the resonator reach their maximum value at a different frequency of switching of the magnetic flux. In the case of a square-wave modulation, the number of excitations is maximum for $\varpi_s = \bar{\omega}_r + \bar{\omega}_0 = 13.75$ GHz. While for the case of a sinusoidal modulation, the maximum is at $\varpi_s = 13.90$ GHz. Moreover, there are no excitations in the system for almost all other values of the frequency of switching of the magnetic flux different from $\varpi_s = \bar{\omega}_r + \bar{\omega}_0$. Fig. 3 shows the time dependence of the number of excitations in the qubit and the resonator for a range of frequencies of switching ϖ_s of the magnetic flux. Since the counter-rotating terms in the Hamiltonian (2), which cause the $|g,0\rangle \to |e,1\rangle$ transition, become relevant for frequency of switching of the coupling equal to the sum frequency of the qubit and resonator transition frequencies, the results of Fig. 3 may seem trivial, but they are instructive. In fact, because of the slight modification of the qubit and cavity transition frequencies during the modulation of the magnetic flux, the sum frequency is not fixed. Indeed, the frequency of switching of the coupling that makes the counter-rotating terms stationary is given by the time average of the sum frequency of the transition frequencies of qubit and resonator. The counter plots in Fig. 3 clearly show that there are no other values of the switching frequency which have any effect on the system. Figs. 3a and 3b depict the results obtained in the case of a square-wave modulation of the magnetic flux, while the results obtained in the case of sinusoidal modulation of the magnetic flux are shown in Figs. 3c and 3d.

It is crucial to note that the state $|e,1\rangle$, where e stands for the qubit in the excited state, can only be reached from the initial state $|g,0\rangle$ through the counter-rotating terms $\hat{a}^\dagger\hat{\sigma}^+ + \hat{a}\hat{\sigma}^-$ in Eq. (11). Since the counter-rotating terms are also responsible for the presence of the Lamb shift, the excitations of the system generated by the nonadiabatic switching "on" and "off" of these terms can be seen as the result of a nonadiabatic change in Lamb shift. Therefore, the dynamical Lamb effect is the main channel of excitation of the qubit and the creation of photons. By considering Hamiltonian (11) in a frame rotating at the qubit and photon's transition frequencies (interaction picture), one has that the counter-rotating terms become dominant over the rotating terms when the qubit/resonator coupling is periodically switched "on" and "off" at a

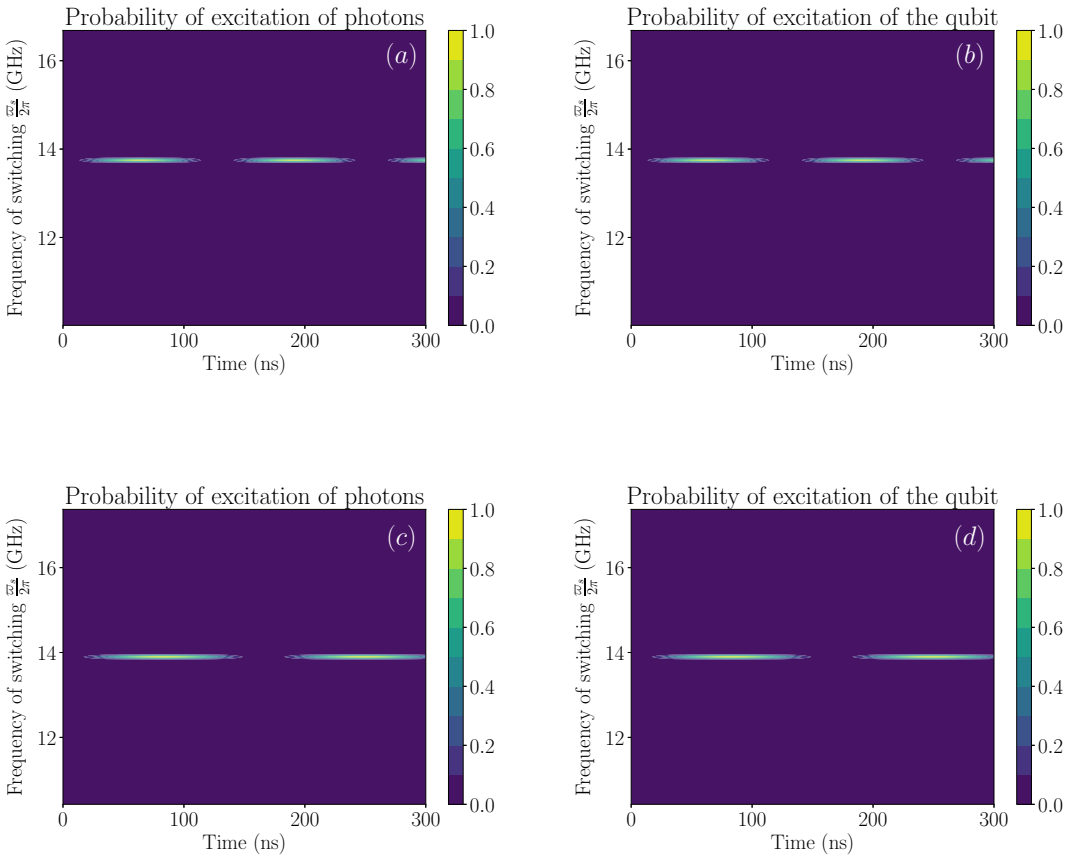

FIG. 3: Time dependence of the number of excitations in the qubit and the number of photons in the resonator for a range of frequencies of switching ϖ_s of the magnetic flux. We take $\varpi_s \in \left[\frac{3}{4}(\bar{\omega}_r + \bar{\omega}_0), \frac{5}{4}(\bar{\omega}_r + \bar{\omega}_0)\right]$. The color-scale in the figures indicates the number of excitations. Expectation value of the number of excitations in the resonator (a) and the qubit (b), for a square-wave modulation of the magnetic flux. Number of photons (c) and probability of excitation of the qubit (d), for a sinusoidal modulation of the magnetic flux.

frequency equal to the sum of the qubit and the resonator time-averaged frequencies. In fact, for the specific modulation of the qubit/resonator coupling chosen the counter-rotating terms become stationary while the rotating terms acquire a phase oscillating at high frequency, thus averaging them to zero. In Ref. [20], it is shown that the interplay between rotating and counter-rotating terms in the Hamiltonian allows for the emission of any number of photons in principle. However, when the contribution of the rotating terms becomes negligible, as in our case, this ceases to be true and only transitions caused by the counter-rotating terms are effectively allowed. So, if we consider a qubit and a resonator initially in the ground state, the transitions $|g,0\rangle \to |e,1\rangle$ and $|e,1\rangle \to |g,0\rangle$, which create and destroy two excitations in the system, respectively, will dominate the dynamics of the system. A comparison of Figs. 3a and 3b, and Figs. 3c and 3d, clearly shows that the number of excitations in the resonator and the qubit coincide and periodically reaches its maximum at one, indicating that the system is undergoing the transitions described above. Experimentally, the state of the qubit can be measured to have an indication of the transition. This is done by using an additional resonator coupled to the qubit. In fact, the resonant frequency of the resonator, and thus its reflection coefficient, depends on the state of the qubit [51]. Although, the coupling of the qubit to the read-out resonator causes a Lamb shift of the energy levels of the qubit, this shift remains constant during the dynamics of the qubit/resonator system described above. Thus, the possibility of generating the nonadiabatic Lamb shift of the qubit needed for the DLE is not affected by the presence of a read-out resonator.

V. CONCLUSION

In conclusion, we predict that the dynamical Lamb effect could arise in superconducting circuits when the coupling of a superconducting qubit with a resonator is periodically switched "on" and "off" nonadiabatically and demonstrate that by using a superconducting circuit which allows to switch between longitudinal and transverse coupling of a qubit to a resonator, it is possible of to observe the dynamical Lamb effect. In particular, the switching between longitudinal and transverse coupling which gives rise to the dynamical Lamb effect is achieved by turning "on" and "off" the magnetic flux through the loops of the superconducting circuit. If the magnetic flux is periodically turned "on" and "off" as a square-wave or a sinusoidal modulation with a frequency of switching equal to the sum of the average qubit and photon transition frequencies, the calculated number of excitations in the qubit and the resonator due to the dynamical Lamb effect reach its maximum values.

Acknowledgments

The authors are grateful to M. Kumph, D. C. Mckay and L. Glazman for the valuable and stimulating discussions.

Appendix A

The analytical expressions of the parameters for the Hamiltonian (11) used in the calculations of the time-evolution of the number of excitations in the qubit and resonator are given in the table below [39].

TABLE II: Expressions of the parameters introduced in Eq. (5).

$\eta(t)=\frac{E_{J1}+E_{J2}}{2k}\left(\frac{2\pi}{\Phi_0}\right)^2 L\cos\left(\frac{\Phi_x(t)}{k}\right)$	$g_{xx}(t)=\frac{E_{J1}-E_{J2}}{2k^2}\sqrt[4]{\frac{2E_C}{E^*_{Jq}(t)}}\frac{\pi}{\Phi_0}\sqrt[4]{\frac{L}{C}\frac{1}{1+\eta(t)}}\cos\left(\frac{\Phi_x(t)}{k}\right)$
$E_c=\frac{e^2}{2C_q+C}$	$g_{zz}(t)=-\frac{E_{J1}-E_{J2}}{16\,k^3}\sqrt{\frac{2E_C}{E^*_{Jq}(t)}}\left(\frac{\pi}{\Phi_0}\right)^2\sqrt{\frac{L}{C}\frac{1}{1+\eta(t)}}\cos\left(\frac{\Phi_x(t)}{k}\right)$
$E^*_{Jq}(t)=E_{Jq}+\left(\frac{\Phi_0}{2\pi}\right)^2\frac{1+\eta(t)}{2L}$	$g_{zx}(t)=-\frac{E_{J1}-E_{J2}}{8\,k^2}\sqrt{\frac{2E_C}{E^*_{Jq}(t)}}\frac{\pi}{\Phi_0}\sqrt[4]{\frac{L}{C}\frac{1}{1+\eta(t)}}\sin\left(\frac{\Phi_x(t)}{k}\right)$
$\omega_r(t)=\sqrt{\frac{1+\eta(t)}{LC}}$	$g_{xz}(t)=-\frac{E_{J1}-E_{J2}}{4\,k^2}\sqrt[4]{\frac{2E_C}{E^*_{Jq}(t)}}\left(\frac{\pi}{\Phi_0}\right)^2\sqrt{\frac{L}{C}\frac{1}{1+\eta(t)}}\sin\left(\frac{\Phi_x(t)}{k}\right)$
$\omega_0(t)=\sqrt{8E_cE^*_{Jq}(t)}-E_c\frac{E_{Jq}+\left(\frac{\Phi_0}{2\pi}\right)^2\frac{\eta(t)}{2k^2L}}{E^*_{Jq}(t)}$	

[1] S. A. Fulling, *Aspects of quantum field theory in curved space-time* (Cambridge Univ. Press, Cambridge, 1989).
[2] H. B. G. Casimir, Proc. K. Ned. Akad. Wet. B **51**, 793 (1948).
[3] H. A. Bethe, Phys. Rev. **72**, 339 (1947).
[4] W. G. Unruh, Phys. Rev. D **14**, 870 (1976).
[5] W. E. Lamb, Jr. and R. C. Retherford, Phys. Rev. **72**, 241 (1947).
[6] M. J. Sparnaay, Physica (Amsterdam) **24**, 751 (1958).
[7] S. K. Lamoreaux, Phys. Rev. Lett. **78**, 5 (1997); **81**, 5475 (1998).
[8] U. Mohideen, Phys. Rev. **81**, 4549 (1998).
[9] B. W. Harris, F. Chen, and U. Mohideen, Phys. Rev. A **62**, 052109 (2000).
[10] H. B. Chan, V. A. Aksyuk, R. N. Kleiman, D. J. Bishop, and F. Capasso, Science **291**, 1941 (2001).
[11] G. Bressi, G. Carugno, R. Onofrio, and G. Ruoso, Phys. Rev. Lett. **88**, 041804(4) (2002).
[12] G. Moore, J. Math. Phys. **11**, 2679 (1970).
[13] N. B. Narozhny, A. M. Fedotov, and Yu. E. Lozovik, Phys. Rev. A **64**, 053807 (2001).
[14] M. O. Scully, V. V. Kocharovsky, A. Belyanin, E. Fry, and F. Capasso, Phys. Rev. Lett. **91**, 243004 (2003).
[15] C. M. Wilson, G. Johansson, A. Pourkabirian, J. R. Johansson, T. Duty, F. Nori, and P. Delsing, Nature **479**, 376 (2011).
[16] P. Lahteenmki, G. S. Paraoanu, J. Hassel, and P. J. Hakonen, Proc. Natl. Acad. Sci. U.S.A. **110**, 4234 (2013).
[17] P. D. Nation, J. R. Johansson, M. P. Blencowe, and F. Nori, Rev. Mod. Phys. **84**, 1 (2012).
[18] D. S. Shapiro, A. A. Zhukov, W. V. Pogosov, and Yu. E. Lozovik, Phys. Rev. A **91**, 063814 (2015).
[19] S. Felicetti, C. Sabìn, I. Fuentes, L. Lamata, G. Romero, and E. Solano, Phys. Rev. B **92**, 064501 (2015).
[20] A. A. Zhukov, D. S. Shapiro, W. V. Pogosov, and Yu. E. Lozovik, Phys. Rev. A **93**, 063845 (2016).
[21] S. V. Remizov, A. A. Zhukov, D. S. Shapiro, W. V. Pogosov, and Yu. E. Lozovik, Phys. Rev. A **96**, 043870 (2017).
[22] O. L. Berman, R. Ya. Kezerashvili, and Yu. E. Lozovik, Phys. Rev. A **94**, 052308 (2016).
[23] M. Amico, O. L. Berman, and R. Ya. Kezerashvili, Phys. Rev. A **96**, 032328 (2017).
[24] M. Amico, O. L. Berman, and R. Ya. Kezerashvili, Phys. Rev. A **98**, 042325 (2018).

[25] C. Sabìn, B. Peropadre, L. Lamata, and E. Solano, Phys. Rev. A **96**, 032121 (2017).
[26] L. García-Àlvarez, S. Felicetti, E. Rico, E. Solano, and C. Sabn, Scientific Reports **7**, 657 (2017).
[27] A. Agustì, E. Solano, and C. Sabn, arXiv:1812.08554 (2018).
[28] G. Benenti, S. Siccardi, and G. Strini, Phys. Rev. A **88**, 033814 (2013).
[29] I. Rabi, Physical Review **49**, 324 (1936).
[30] S. DeLiberato, C. Ciuti, and I. Carusotto, Phys. Rev. Lett. **98**, 103602 (2007).
[31] C. Ciuti, G. Bastard, and I. Carusotto, Phys. Rev. B **72**, 115303 (2005).
[32] C. Ciuti and I. Carusotto, Phys. Rev. A **74**, 033811 (2006).
[33] S. DeLiberato, D. Gerace, I. Carusotto, and C. Ciuti, Phys. Rev. A **80**, 053810 (2009).
[34] R. Stassi, A. Ridolfo, O. DiStefano, M. J. Hartmann, and S. Savasta, Phys. Rev. Lett. **110**, 243601 (2013).
[35] V. Gramich, P. Solinas, M. Möttönen, J. P. Pekola, and J. Ankerhold, Phys. Rev. A **84**, 052103 (2011).
[36] V. Gramich, S. Gasparinetti, P. Solinas, and J. Ankerhold, Phys. Rev. Lett. **113**, 027001 (2014).
[37] M. Silveri, *et al.*, Nature Physics, DOI: https://doi.org/10.1038/s41567-019-0449-0 (arXiv:1809.00822) (2019).
[38] S. Richer and D. DiVincenzo, Phys. Rev. B **93**, 134501 (2016).
[39] S. Richer, N. Maleeva, S. T. Skacel, I. M. Pop, and D. DiVincenzo, Phys. Rev. B **96**, 174520 (2017).
[40] G. Vidal and R. Tarrach, Phys. Rev. A **59**, 141-155, (1999).
[41] Y. Chen, C. Neill, P. Roushan, N. Leung, M. Fang, R. Barends, J. Kelly, B. Campbell, Z. Chen, B. Chiaro, A. Dunsworth, E. Jeffrey, A. Megrant, J. Y. Mutus, P. J. J. O'Malley, C. M. Quintana, D. Sank, A. Vainsencher, J. Wenner, T. C. White, M. R. Geller, A. N. Cleland, and J. M. Martinis, Phys. Rev. Lett. **113**, 220502 (2014).
[42] D. C. McKay, S. Filipp, A. Mezzacapo, E. Magesan, J. M. Chow, and J. M. Gambetta, Phys. Rev. Appl. **6**, 064007 (2016).
[43] M. Roth, M. Ganzhorn, N. Moll, S. Filipp, G. Salis, and S. Schmidt, Phys. Rev. A **96**, 062323 (2017).
[44] Y. Lu, S. Chakram, N. Leung, N. Earnest, R.K. Naik, Ziwen Huang, P. Groszkowski, E. Kapit, J. Koch, and D. I. Schuster, Phys. Rev. Lett. **119**, 150502 (2017).
[45] Q.-K. He and D. L. Zhou (2018) arXiv:1805.10794.
[46] P. M. Billangeon, J. S. Tsai, and Y. Nakamura, Phys. Rev. B **91**, 094517 (2015).
[47] I. G. Lang and Y. A. Firsov, Soviet Physics JETP **16**, 1301 (1963).
[48] M. H. Devoret, *Quantum Fluctuations in Electrical Circuits*. In S. Reynaud, E. Giacobino, and J. Zinn-Justin, editors, Fluctuations Quantiques/Quantum Fluctuations, page 351 (1997).
[49] J. Clarke, A. N. Cleland, M. H. Devoret, D. Esteve, and J. M. Martinis, Science 239, 992 (1988).
[50] J. M. Martinis, S. Nam, J. Aumentado, and C. Urbina, Phys. Rev. Lett. 89, 117901 (2002).
[51] Y. Makhlin, G. Schön, and A. Shnirman, Rev. Mod. Phys., **73**, 357 (2001).